

ENC-2022-0413

EFFECT OF THE GEOMETRY ON THE PERFORMANCE OF A SMALL-SCALE SOLAR CHIMNEY

Cristiana Brasil Maia

Janaína de Oliveira Castro Silva

Pontifícia Universidade Católica de Minas Gerais, Av. Dom José Gaspar, 500, 30535-901 – Belo Horizonte – MG

E-mail: cristiana@pucminas.br, janainajocs@hotmail.com

Abstract. *The world population is increasing, together with an increase in consumption patterns. Conventional energy sources will not be able to fulfill the global energy demand in a few years. Renewable sources play an important role to provide energy, as they are inexhaustible and environmentally friendly. Solar energy is one of the most promising renewable energy sources, considering its technology, improvements, and fast development. Solar chimneys use the incident solar energy to generate a hot airflow, that can be used to generate electricity or to dry agricultural products, and also to produce freshwater. In the design of a solar chimney, it is important to evaluate the influence of the ambient conditions and geometry on its performance. The present work aims to present the effect of the main geometric parameters on the airflow characteristics. The ambient temperature and incident solar radiation were predicted for the city of Belo Horizonte, Brazil, and, based on them, the mass flow rates and the temperatures of the airflow and the ground surface were determined. The heat transfer rates and energy and exergy efficiencies were estimated for the device. The analysis was performed for a 1-h interval, for a whole year, and average values were obtained for different geometries. The influence of the tower diameter and the collector diameter and height can be evaluated. It was observed that the mass flow rate increases with the tower diameter and height and decreases with the collector height, and also that the tower diameter is the most important design parameter, with greater effect on the performance of the system.*

Keywords: *Solar chimney, analytical model, modular solar chimney, geometry modification.*

1. INTRODUCTION

Solar energy is a clean, renewable and abundant energy source. It can be divided into active and passive applications. The main difference between active and passive solar is that passive heating uses solar energy to heat objects and spaces, and active heating uses solar radiation as a source of thermal energy to heat fluids and generate mechanical or electric power. The active applications are subdivided into CSP (concentrated solar power), photovoltaics, and solar thermal heating.

The solar chimney is a device included in the third application, of thermal heating. It uses the incident solar energy to generate a hot airflow, that can be used to produce electricity (Schlaich, 2002) or to dry agricultural products (Maia *et al.*, 2017). It comprises a solar collector, a tower, and when generating power, a turbine. The ground under the translucent solar collector is heated by solar energy, which heats the air. Buoyancy forces drive a continuous flow into the tower located in the middle of the collector. A turbine located in the path of the airflow converts the kinetic energy into electricity (Koonsrisuk, 2012).

Since the first prototype was built, in 1982 (Murena, Gaggiano and Mele, 2022), several works were published with analytical (Koonsrisuk, 2012; Setareh, 2021), numerical (Gholamalizadeh and Kim, 2016; Murena, Gaggiano and Mele, 2022) and experimental (Ghalamchi, Kasaeian and Ghalamchi, 2015; Krumar Mandal *et al.*, 2022) studies, for power generation only, drying only or combined with other purposes, such as PV, geothermal, solar ponds, and desalination, as described by (Ahmed *et al.*, 2022).

It was demonstrated that large dimensions are required to generate power at competitive prices (Maia and Castro Silva, 2022). Small-scale devices can be used to dry agricultural products (Maia *et al.*, 2013) or to experimentally evaluate the influence of the geometry on the performance of the device (Balijepalli, Chandramohan and Kirankumar, 2020).

In the design of a solar chimney, it is important to assess the influence of the ambient conditions and geometry on its performance. Most of the works published use fixed values of solar radiation, ambient temperature and mass flow rate

to evaluate the performance of the solar chimney. Also, steady-state conditions are commonly assumed. In this paper, a mathematical model is used to predict the solar radiation and ambient temperature for the city of Belo Horizonte, Brazil. The ambient conditions are used as input data to predict the ground surface and outlet temperatures, the mass flow rate and the heat transfer rate to the airflow, as well as energy and exergy efficiencies of the solar chimney. The simulation was run for a 1-h interval, for a whole year. Monthly-averaged results were compared to different geometric parameters, to evaluate the influence of the geometry on the performance of the system.

2. MATERIALS AND METHODS

Figure 1 illustrates the schematics of a solar chimney. As shown, it comprises two principal parts: the collector and the chimney. The dimensions of the standard geometry are the same of a prototype built in Belo Horizonte, Brazil.

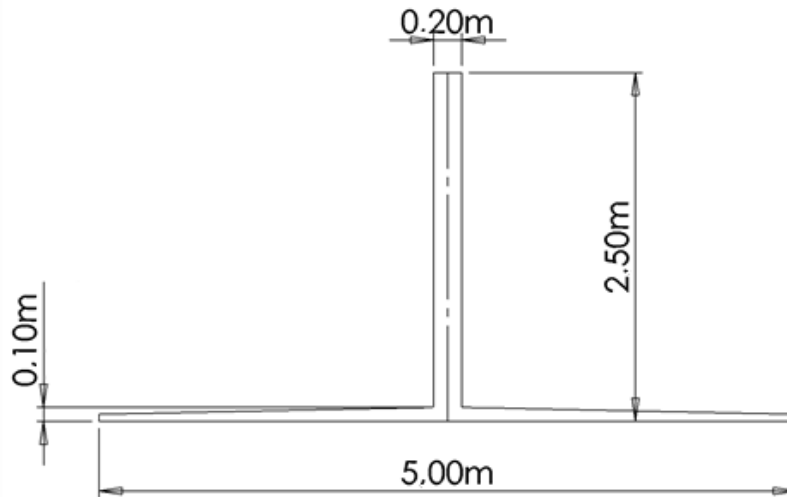


Figure 1. Schematics of the solar chimney.

An energy balance was developed for the solar chimney, and the heat transfer rates are shown in Figure 2.

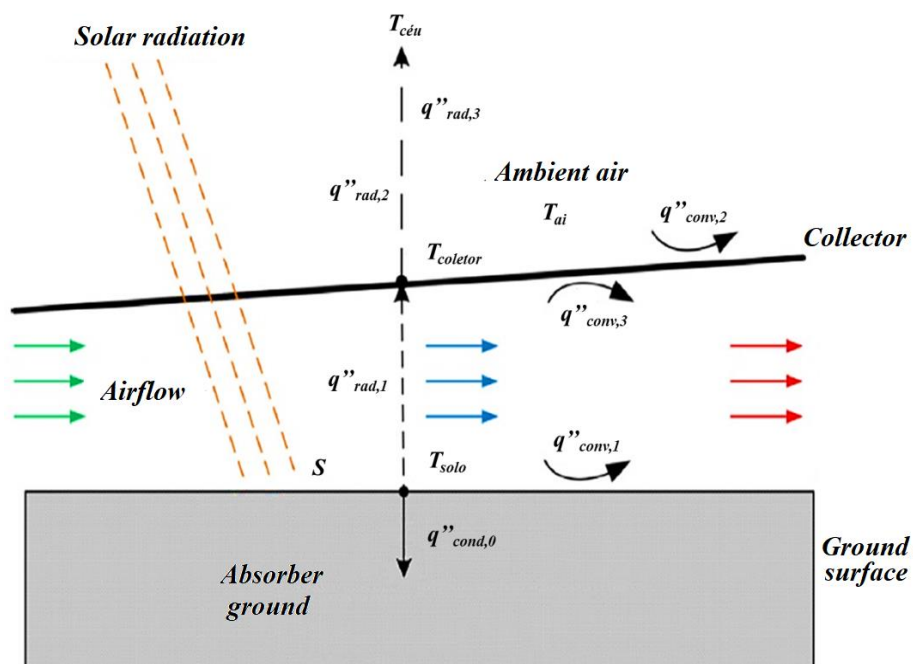


Figure 2. Energy balance.

The convective heat transfer from the airflow ($q''_{conv,3}$) and the radiative heat transfer from the ground surface ($q''_{rad,1}$) to the collector surface are lost to the environment by convection ($q''_{conv,2}$) and radiation ($q''_{rad,2}$). The energy transferred by the ground surface to the deeper layers by conduction ($q''_{cond,0}$) is given by the difference between the absorbed portion (S) of the incident solar energy, the convection heat transfer to the airflow ($q''_{conv,1}$), and the radiative heat transfers to the collector ($q''_{rad,1}$) and to the environment ($q''_{rad,3}$), as shown in Eq. (1).

$$S - q''_{conv,1} - q''_{rad,1} - q''_{rad,3} = q''_{cond,0} \quad (1)$$

The absorbed portion of the solar energy S is given by (Duffie and Beckman, 2013)

$$S = I_b R_b (\tau\alpha)_b + I_d R_d \left(\frac{1 + \cos\beta}{2} \right) + \rho_g I (\tau\alpha)_g \left(\frac{1 - \cos\beta}{2} \right) \quad (2)$$

I is the total incident irradiation, given by the sum of the beam (I_b), diffuse (I_d), and ground-reflected components. $(\tau\alpha)$ is the transmittance-absorptance product for the beam (subscript b), diffuse (subscript d), and ground-reflected (subscript g) components. β represents the angle between the collector and a horizontal surface and ρ_g is the ground reflectance. R_b represents the ratio between the radiation incident on a tilted surface and on a horizontal surface.

The heat transfer rates are modeled according to the literature. A complete description of the model is found in (Maia and Castro Silva, 2022).

The ground surface temperature T_{ground} is given by (Maia, 2005)

$$T_{ground}(t) = T_i + \frac{2}{\sqrt{\pi}} \frac{\alpha'}{k_g} \int_{t'=0}^t \frac{q''_{cond,0}(t')}{\sqrt{4\alpha'(t-t')}} dt' \quad (11)$$

α' and k_g are the ground thermal diffusivity and conductance, respectively.

The mass flow rate is predicted by an adaptation of an expression proposed by (Koonsrisuk, Lorente and Bejan, 2010), considering small-scale dimensions of the solar chimney. q''_{disp} represents the energy available for the airflow.

$$\dot{m} = \sqrt[3]{\frac{\rho^2 \beta' g q''_{disp} \pi^3}{8 C p_{ao}} H_t R_c^2} \sqrt{\frac{4f H_t}{D_t^5} + \frac{F_x}{64 R_c h_c^3} + \frac{1}{D_t^4}} \quad (16)$$

F_x and F_y represent the friction factors of the collector and tower, respectively, given by (Koonsrisuk, Lorente and Bejan, 2010):

The outlet airflow temperature is given by (Koonsrisuk, Lorente and Bejan, 2010)

$$T_{ao} = \frac{q''_{conv,1} \pi}{\dot{m} C_p} \left[R_c^2 - \left(\frac{D_t}{2} \right)^2 \right] + T_{ai} \quad (18)$$

The total heat transfer rate to the airflow is determined through a global energy balance of the airflow

$$\dot{Q} = \dot{m} \left(h_{ao} - h_{ai} + \frac{V_{ao}^2}{2} - \frac{V_{ai}^2}{2} \right) \quad (21)$$

h_{ao} and h_{ai} represent, respectively, the specific enthalpy of the airflow at the outlet and inlet.

According to (Nizetic, Ninic and Klarin, 2008), the energy efficiency of a solar chimney is

$$\eta_{SP} = \eta_{col} \eta_{cs} = \left[\frac{\int \dot{m} c_p (T_{ao} - T_{ai}) dt}{A_{col} H_0} \right] \left[\frac{H_t g}{C_p T_{ai}} \right] \quad (22)$$

The exergy efficiency is (Celma and Cuadros, 2009):

$$\varepsilon = 1 - \frac{\dot{E}x_{lost}}{\dot{E}x_e} \quad (33)$$

$\dot{E}x_{lost}$ is the lost exergy rate and $\dot{E}x_e$ is the exergy rate at the inlet.

3. RESULTS

Simulations were performed on an hourly basis, for each day of the year. The results are presented in a monthly average for the inlet, outlet, and ground surface temperatures, the heat transferred to the fluid, the mass flow rate, and the energy and exergy efficiencies. The monthly averaged results for the ambient conditions are also presented. Figure 3 presents the energy absorbed by the ground surface and the ambient temperature. As expected, the values decrease from January to July and increase from July to December, consistent with the seasons.

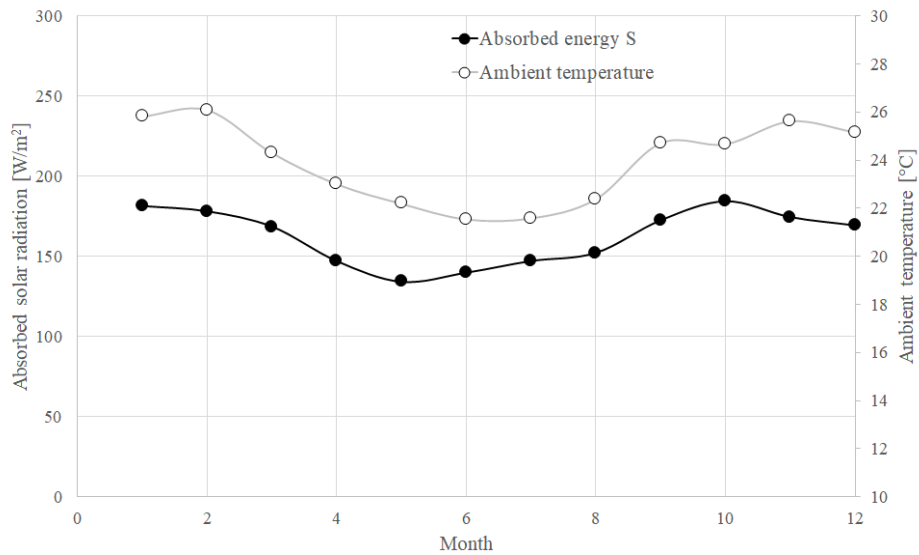


Figure 3. Ambient conditions on a monthly averaged basis.

The temperatures are presented in Figure 4. The air enters the device at ambient temperature and is heated by the ground surface, increasing its temperature. Therefore, the ground surface temperature is higher than the outlet temperature, which is higher than the inlet temperature. On average, the temperature rise of the airflow was 4°C, for an average difference between the ground surface and outlet airflow temperatures of 8°C. It is worth noting, however, that these are average values, with higher differences found when evaluating the hourly values. Concerning the annual variation, the behavior is similar to ambient temperature and solar radiation (Fig. 3), decreasing from January to July and increasing from July to December.

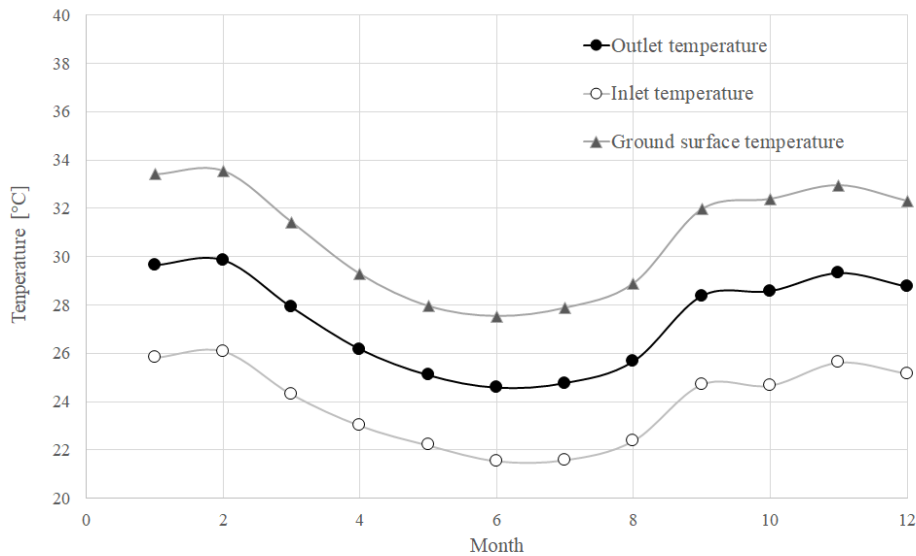


Figure 4. Temperature distribution on a monthly averaged basis.

The monthly averaged mass flowrate did not present significant variations throughout the year (Figure 5), with an average value of 0.025 kg/s. When considered hourly values, it can be seen that the hourly variation is higher. The heat transfer rates to the airflow showed similar behavior to the solar radiation, higher in the winter and lower in the summer. The annual average was approximately 0.45 kW.

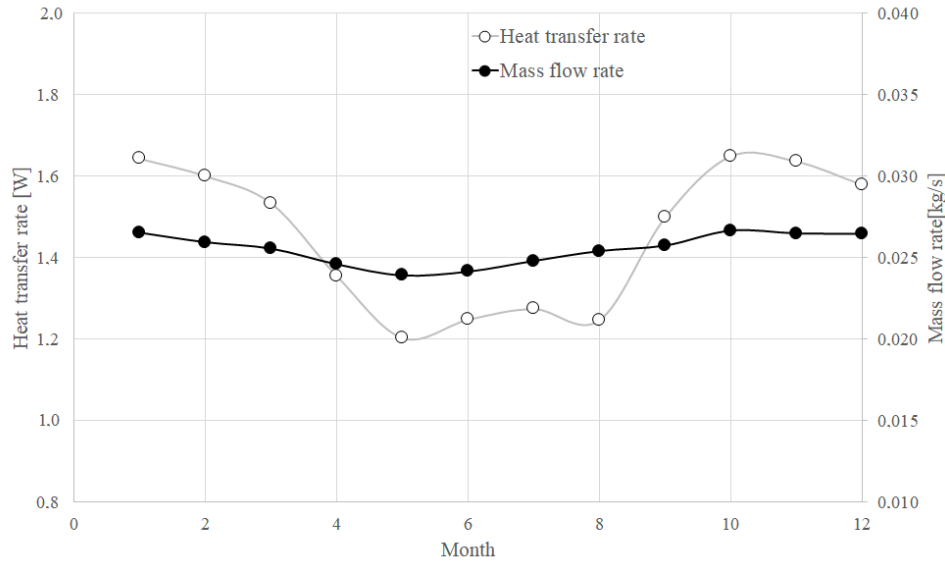


Figure 5. Airflow parameters on a monthly averaged basis

Figure 6 presents the energy and exergy efficiencies. The values are small, consistent with the literature. The average energy efficiency was 0.01% and the exergy efficiency was 11%. As expected, the exergy efficiency is higher than the energy efficiency.

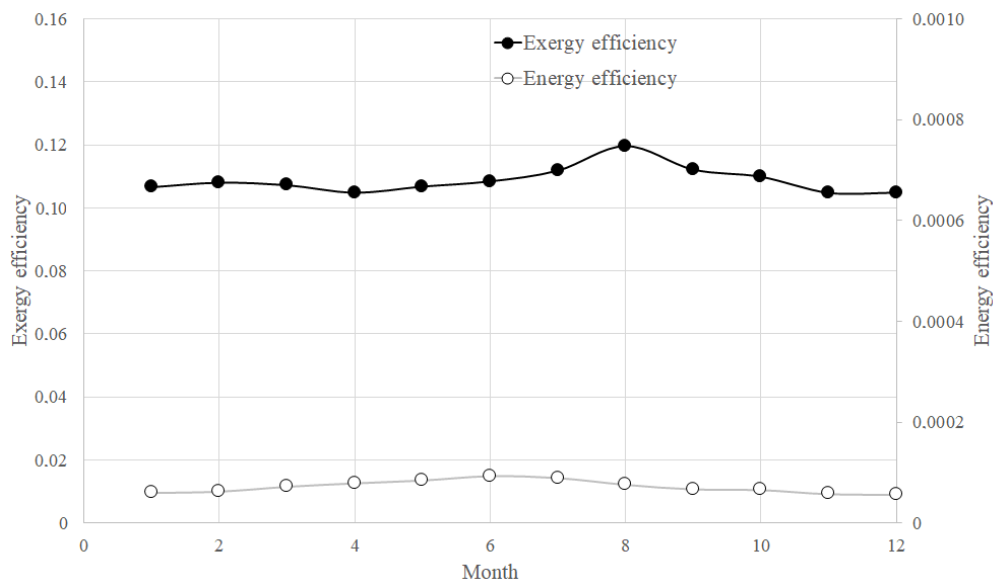


Figure 6. Energy and exergy efficiencies on a monthly averaged basis.

Once assessed the annual behavior of the main airflow parameters, the influence of the geometric dimensions on the performance of the solar chimney was evaluated. Figure 7 presents the variation of the parameters with a variation of the collector diameter from 2.0 to 5.0 m. The ground surface and outlet temperatures varied only slightly with the collector diameter, with maximum variations of 0.3°C and 1.3°C, respectively. The mass flow rate and the heat transfer rate increased with the collector diameter, due to the higher area in which the solar radiation is absorbed by the ground. The average mass flow rate increased from 0.012 (Dc = 2.0 m) to 0.026 kg/s (Dc = 5.0 m). The energy efficiency increased with the collector diameter, but the exergy efficiency did not present a trend.

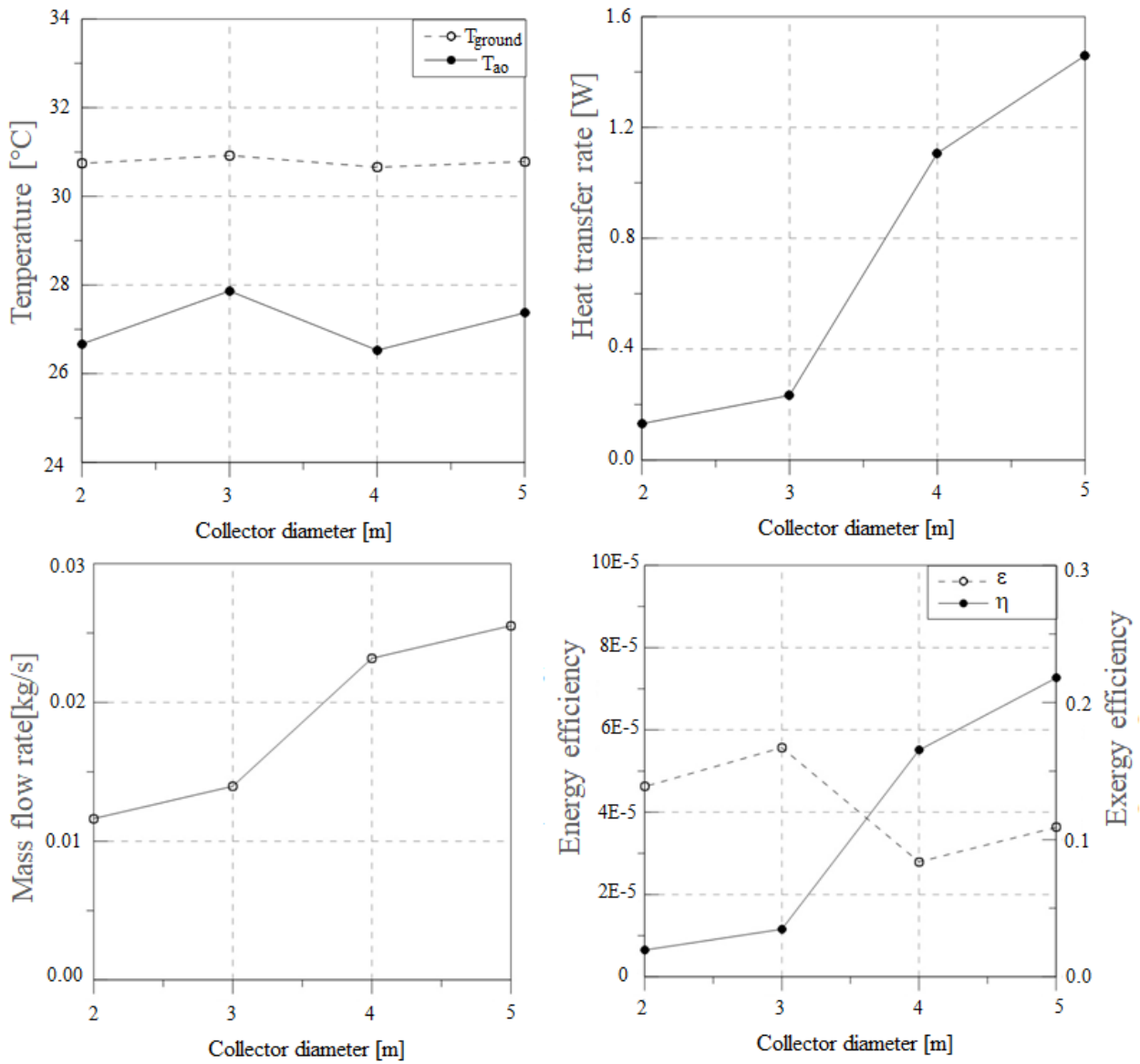


Figure 7. Influence of the collector diameter.

The influence of the tower diameter on the performance of the system is shown in Figure 8, for a variation from 0.05 m to 2.0 m. It was observed that the ground surface and outlet temperatures decreased with the tower diameter, with a maximum variation of the outlet temperature of 31.5°C. The mass flow rate and the heat transfer rate also decreased with the tower diameter. The efficiencies showed opposite behaviors, with the exergy efficiency decreasing and the energy efficiency increasing. The maximum exergy efficiency was 22.4%.

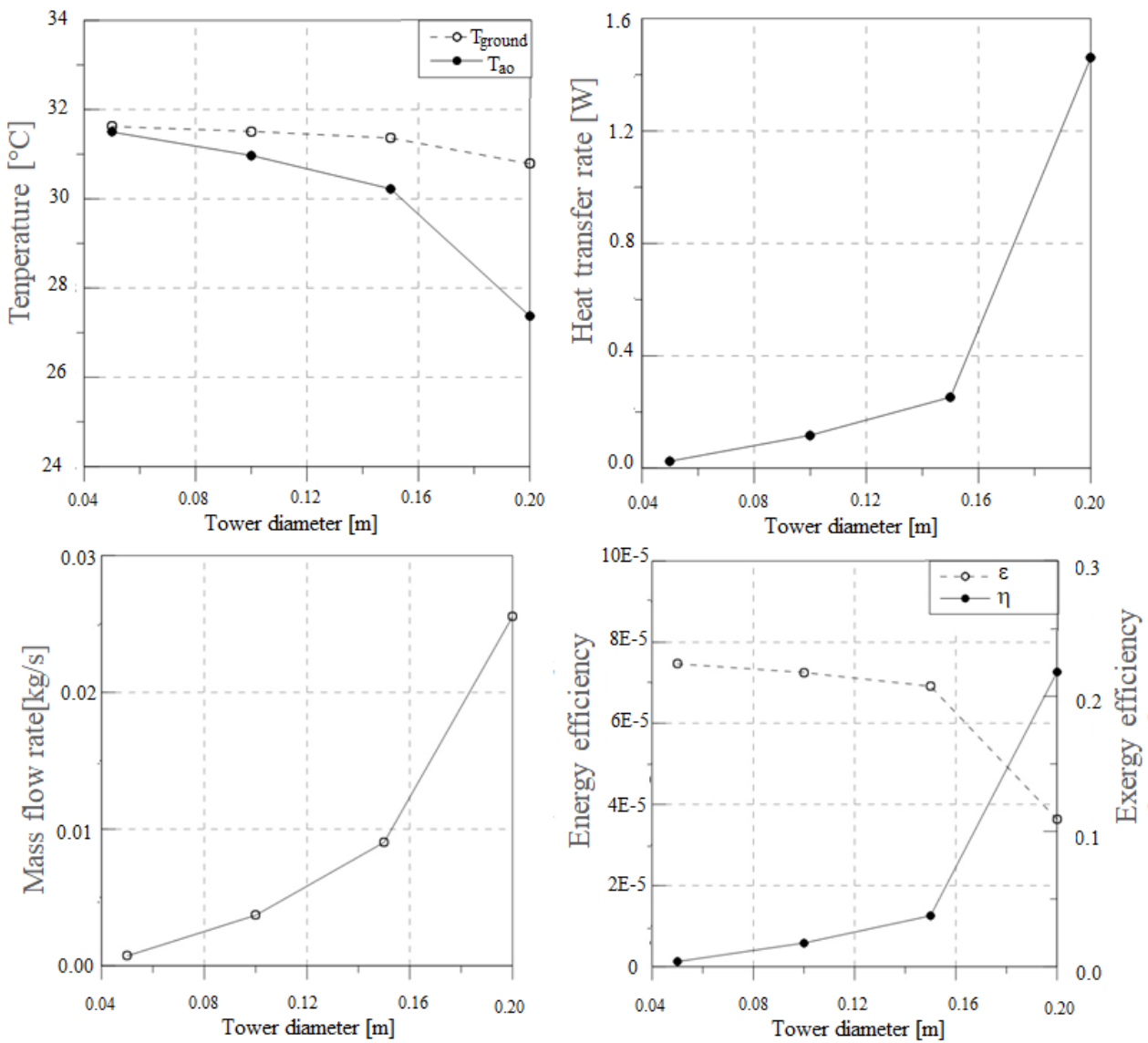


Figure 8. Influence of the tower diameter.

The tower height varied from 1.0 m to 2.5 m (Figure 9). The ground surface and outlet temperatures, as well as the heat transfer rate and the exergy efficiency, did not change significantly. The mass flow rate, on the other hand, increased with the tower height. The increase in the tower height increased the pressure difference between the bottom and the top of the tower, increasing the driving force of the airflow. The energy efficiency increased with the tower height.

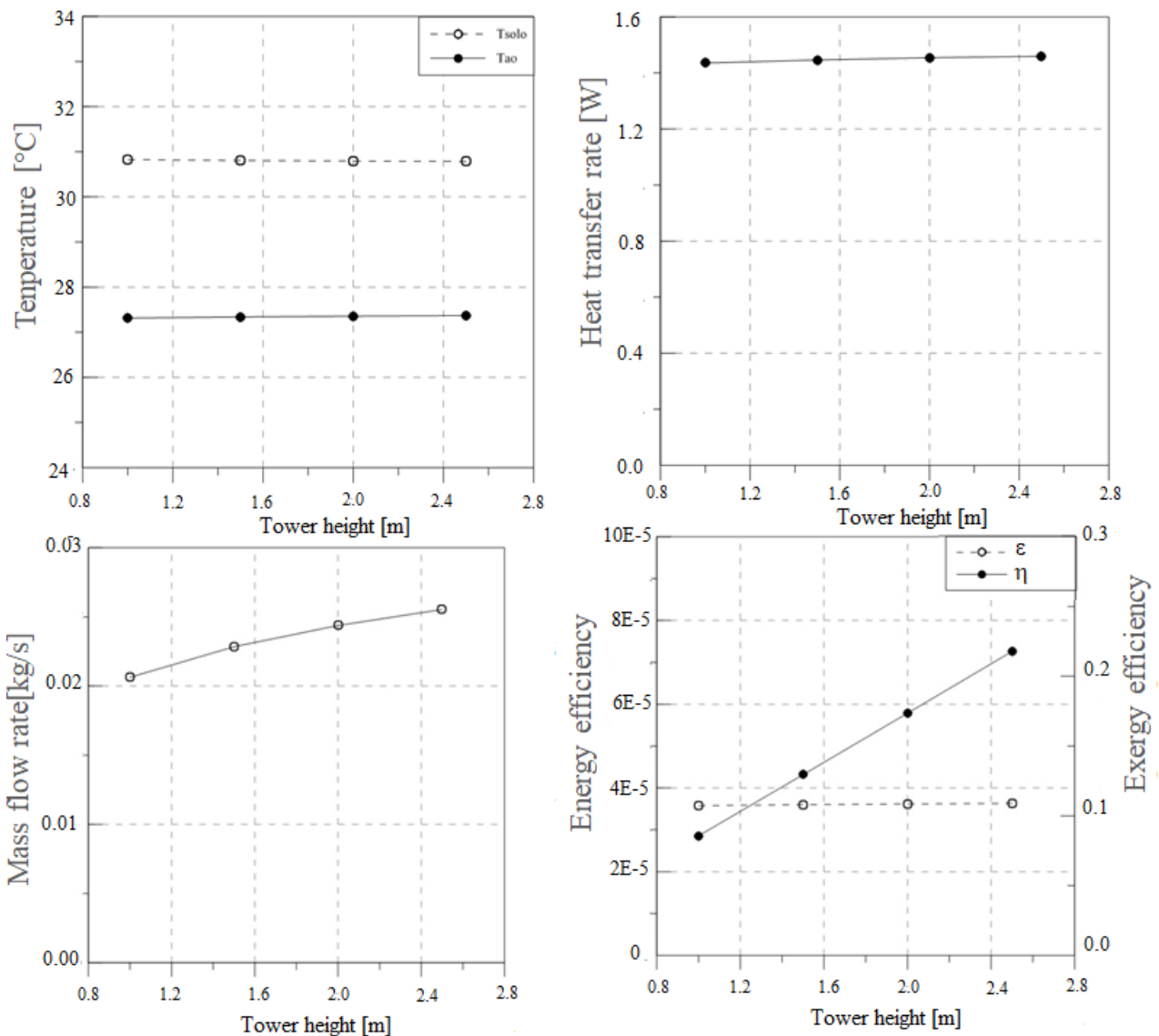


Figure 9. Influence of the tower height.

In a summary, it can be seen that the geometric parameters with higher influence on the heat transfer and mass flow rates are the collector diameter and the tower diameter. In general, an increase in the dimensions of the system led to an increase in the energy efficiency of the system.

4. CONCLUSIONS

In this paper, it was developed a mathematical model to predict the airflow parameters inside a small-scale solar chimney. The analysis was performed on an hourly basis, and the results were presented on a monthly-averaged basis. The ambient conditions (solar radiation and ambient temperature) were predicted for Belo Horizonte, Brazil. They were used as input data to evaluate the airflow temperatures, mass flow rate, and heat transfer rate, used to determine the energy and exergy efficiencies.

For a given geometry, it was evaluated the behavior of the airflow throughout the year. From January to July, the ambient temperature and solar radiation decreased, and the airflow temperatures and heat transfer rates followed this behavior. From July to December, the values increased. As expected, the ground surface temperature is higher than the outlet airflow temperature, which is higher than the ambient temperature.

A parametric analysis was performed, varying the main geometric parameters to evaluate its influence on the performance of the solar chimney. The collector diameter and the tower diameter showed greater impact on the airflow parameters, for the range of values evaluated. It was shown that the heat transfer rate and the mass flow rate increased with the increase in the dimensions of the solar chimney. The energy efficiency also increased with the dimensions.

5. ACKNOWLEDGEMENTS

This study was financing in part by the Coordenação de Aperfeiçoamento de Pessoal de Nível Superior - Brasil (CAPES) – Finance Code 001. The authors are also thankful to PUC Minas, FAPEMIG, and CNPq.

6. REFERENCES

- Ahmed, O. K. *et al.* (2022) ‘Hybrid solar chimneys: A comprehensive review’, *Energy Reports*. doi: 10.1016/j.egy.2021.12.007.
- Balijepalli, R., Chandramohan, V. P. and Kirankumar, K. (2020) ‘Development of a small scale plant for a solar chimney power plant (SCPP): A detailed fabrication procedure, experiments and performance parameters evaluation’, *Renewable Energy*. doi: 10.1016/j.renene.2019.12.001.
- Celma, A. R. and Cuadros, F. (2009) ‘Energy and exergy analyses of OMW solar drying process’, *Renewable Energy*, 34(3), pp. 660–666. doi: 10.1016/j.renene.2008.05.019.
- Duffie, J. A. and Beckman, W. A. (2013) *Solar Engineering of Thermal Processes: Fourth Edition*, *Solar Engineering of Thermal Processes: Fourth Edition*. doi: 10.1002/9781118671603.
- Ghalamchi, Mehran, Kasaeian, A. and Ghalamchi, Mehrdad (2015) ‘Experimental study of geometrical and climate effects on the performance of a small solar chimney’, *Renewable and Sustainable Energy Reviews*, pp. 425–431. doi: 10.1016/j.rser.2014.11.068.
- Gholamalizadeh, E. and Kim, M. H. (2016) ‘CFD (computational fluid dynamics) analysis of a solar-chimney power plant with inclined collector roof’, *Energy*, 107. doi: 10.1016/j.energy.2016.04.077.
- Koonsrisuk, A. (2012) ‘Mathematical modeling of sloped solar chimney power plants’, *Energy*, 47(1). doi: 10.1016/j.energy.2012.09.039.
- Koonsrisuk, A., Lorente, S. and Bejan, A. (2010) ‘Constructal solar chimney configuration’, *International Journal of Heat and Mass Transfer*, 53(1–3), pp. 327–333. doi: 10.1016/j.ijheatmasstransfer.2009.09.026.
- Krumar Mandal, D. *et al.* (2022) ‘Experimental investigation of a solar chimney power plant and its numerical verification of thermo-physical flow parameters for performance enhancement’, *Sustainable Energy Technologies and Assessments*, 50, p. 101786. doi: 10.1016/j.seta.2021.101786.
- Maia, C. B. (2005) *Análise Teórica e Experimental de uma Chaminé Solar: Avaliação Termofluidodinâmica*. Universidade Federal de Minas Gerais.
- Maia, C. B. *et al.* (2013) ‘Energy and exergy analysis of the airflow inside a solar chimney’, *Renewable and Sustainable Energy Reviews*. Elsevier, 27, pp. 350–361. doi: 10.1016/j.rser.2013.06.020.
- Maia, C. B. *et al.* (2017) ‘Thermodynamic analysis of the drying process of bananas in a small- scale solar updraft tower in Brazil’, *Renewable Energy*, 114, pp. 1005–1012. doi: 10.1016/j.renene.2017.07.102.
- Maia, C. B. and Castro Silva, J. de O. (2022) ‘Thermodynamic assessment of a small-scale solar chimney’, *Renewable Energy*. Elsevier Ltd, 186, pp. 35–50. doi: 10.1016/j.renene.2021.12.128.
- Murena, F., Gaggiano, I. and Mele, B. (2022) ‘Fluid dynamic performances of a solar chimney plant: Analysis of experimental data and CFD modelling’, *Energy*, 249. doi: 10.1016/j.energy.2022.123702.
- Nizetic, S., Ninic, N. and Klarin, B. (2008) ‘Analysis and feasibility of implementing solar chimney power plants in the Mediterranean region’, *Energy*, 33(11), pp. 1680–1690. doi: 10.1016/j.energy.2008.05.012.
- Schlaich, J. (2002) *The Solar Chimney: electricity from the Sun*. Stuttgart.
- Setareh, M. (2021) ‘Comprehensive mathematical study on solar chimney powerplant’, *Renewable Energy*, 175. doi: 10.1016/j.renene.2021.05.017.

7. RESPONSIBILITY NOTICE

The authors are the only responsible for the printed material included in this paper.